Deposition of Potential Energy in Solids by Slow, Highly Charged Ions

T. Schenkel,* A. V. Barnes, T. R. Niedermayr, M. Hattass, M. W. Newman,
G. A. Machicoane, J. W. McDonald, A. V. Hamza, and D. H. Schneider
University of California, Lawrence Livermore National Laboratory, Livermore, California 94550
(Received 28 January 1999)

We have measured the deposition of potential energy of slow ($\sim 6 \times 10^5$ m/s), highly charged ions in solids with an ion implanted silicon detector. A large fraction (about 35% or 60 keV) of the potential energy dissipated by Au^{69+} ions can be traced in electronic excitations deep (>50 nm) inside the solid. In contrast, only about 10% of the potential energy has been accounted for in measurements of emitted secondary particles.

PACS numbers: 34.50.Dy, 31.50.+w, 72.30.+q, 78.90.+t

The potential energy of slow ($v < 10^6$ m/s), very highly charged ions (SHCI) is the sum of the binding energies of the electrons that were removed when forming the ion [1,2]. Earlier studies have shown that SHCI-like Xe^{52+} and Au^{69+} reach charge state equilibrium after traveling in solids for only about 5–10 fs [3]. During this short time, all their potential energy, e.g., 169.6 keV for Au^{69+}, is dissipated. Detailed knowledge of deexcitation dynamics and the response of solids to intense, ultrafast electronic excitation from SHCI is important for the development of novel techniques for materials analysis [4] and modification on a nanometer scale [5]. So far, the quantitative differentiation of energy dissipation channels has been addressed solely in measurements of emitted secondary electrons and ions, photons, and excited plasmons. Surprisingly, only about 10% of the available potential energy of very highly charged ions could be traced in low energy electrons [6–9], Auger electrons [2,6,9], plasmons [9], x-rays [1,10], and secondary ions [7,11]. In this Letter we report on the first measurements of potential energy deposition into electronic excitations of target material. For Au^{69+} and Xe^{52+} about 35% to 40% of the potential energy is traced more than 50 nm deep in a silicon target.

Highly charged ions were extracted from the Electron Beam Ion Trap (EBIT) at Lawrence Livermore National Laboratory [1] and reached the target chamber after momentum analysis in a 90° bending magnet. The pressure in the scattering chamber was kept below 10^{-8} torr. SHCI impinged on an ion implanted and passivated silicon detector [12,13] at normal incidence. The 50 nm thick, inactive, front contact layer of the detector consisted of a thin SiO_2 layer followed by a layer of silicon that had been implanted with a high concentration of boron. The depletion region had a nominal depth of 100 μm, much larger than the range of projectiles, which was only a few hundred nanometers. Most of the potential energy of projectiles is initially deposited in the inactive contact layer of the detector and eventually spreads into the depletion region. Low energy electrons, originating from cascade multiplication of Auger electrons in the contact layer, diffuse into the sensitive detector volume [14] and constitute the dominant contribution to the collected charge. In addition, UV photons and x rays that are emitted into the solid angle of the detector ($\sim 2\pi$) by deexciting SHCI can be absorbed in the depletion region. Absorption of energetic photons results in electron-hole pair production. Electrons are swept to the back electrode in the applied electric field; here they are collected and contribute to the measured pulse height distributions. The front contact of the silicon detector was grounded, and electrons were collected at the positively biased rear electrode. The detector was operated under bias conditions where charge collection was saturated. Signals were amplified using standard electronics consisting of a charge sensitive preamplifier and a spectroscopic amplifier. Detector and electronics were operated at room temperature. For determination of contributions from kinetic energy loss, we prepared projectiles in charge-state equilibrium by transmitting SHCI through thin carbon foils before they reached the detector [1,3]. Here, a negative bias was applied to the foil targets for compensation of energy loss in the foils so that charge equilibrated and highly charged projectiles reached the detector surface with the same kinetic energy [3].

Most experiments in SHCI-solid interactions have focused on secondary particle emission into the vacuum. The experiment described here probes the deposition of potential energy in the bulk of the target material.

We calibrated the silicon detector using a set of alpha-particle sources with known energies in the 4–5 MeV range. Since kinetic energies of SHCI were much lower (i.e., 0.2 to 1 MeV), we further calculated contributions of electronic energy loss to the stopping of slow, heavy ions in silicon by SRIM [15]. In these calculations, energy loss in the contact layer, the contribution of elastic collisions to stopping in the active device volume, and a contribution to target ionization from energetic recoils were included. The observed detector response, i.e., average number of collected electrons or the mean pulse heights, for oxygen, xenon, and gold projectiles in charge state equilibrium scaled linearly with calculated values for electronic energy loss in the sensitive device volume. Results from calculations and the calibration with alpha sources were consistent. In a conservative estimate, the absolute uncertainty of the energy calibration is about 20%.

In Fig. 1, we show pulse height distributions from the ion implanted silicon detector responding to the impact of gold ions in charge state equilibrium ($Au^{q_{eq}+}$, $q_{eq} \approx 1.6+$) and Au^{69+} ($E_{pot} = 169.6$ keV) where the kinetic energies were kept constant at 447 keV. The mean pulse height is significantly increased due to deposition of potential energy by Au^{69+} ions.

In Fig. 2, values for mean pulse heights are shown vs potential energies of projectiles. Mean pulse heights were calculated from measured pulse height distributions. A value of 5% for the typical statistical error is included. Projectiles were $Xe^{22,32,44,52+}$ ($E_{pot} = 6.0$, 19.3, 51.3, and 121 keV), and $Au^{42,52,64,69+}$ ($E_{pot} = 31.1$, 58.8, 130.2, and 169.6 keV) with kinetic energies of 308 and 447 keV for xenon (open diamonds) and gold ions (solid diamonds), respectively. The kinetic energies were selected so that the velocity of ions from both species was the same ($v = 6.6 \times 10^5$ m/s $\approx 0.3 v_{Bohr}$). At zero potential energy, we include pulse heights for projectiles in charge state equilibrium and at the same kinetic energies. The increase of mean pulse heights as a function of potential energy demonstrates that a large fraction of the potential energy can be traced deep (>50 nm) in the bulk of the target material. We now discuss the energy dissipation processes that contribute to this result.

The total energy of a projectile is the sum of its kinetic, E_{kin}, and potential energies, E_{pot}. Projectiles travel first through the 50 nm thick insensitive layer, consisting of a thin (i.e., few nm thick) SiO_2 passivation layer and a heavily boron doped silicon contact layer, before they reach the depletion region of the detector. Ions with velocities used in this study travel only about 5 nm into the target during the equilibration time of 5–10 fs [3]. The loss of kinetic energy in the contact layer during deexcitation is a function of the projectile charge state [3], $E_c = E_c(q)$, and preequilibrium energy-loss enhancements have to be considered when calculating the contribution to measured pulse heights from kinetic energy loss [16]. Deexcitation of SHCI already begins a few nanometers above the target surface with the formation of hollow atoms [2]. However, only a small fraction (<5%) of the potential energy is dissipated above the surface [6,8]. This is the case because the available time is limited by the ion velocity [8], and rates for Auger and radiative transitions are not high enough. When SHCI reach the surface, electrons in high Rydberg states ($n > 10$) are "peeled off" by target electrons [1,2], and a more compact screening cloud of electrons forms a hollow atom inside the solid. Silicon valence electrons resonantly populate the $n \approx 5-8$ levels in gold projectiles that started out as Au^{69+}. Direct population of levels in the N and O shells of hollow gold atoms by core electrons of silicon is possible only in relatively rare small impact parameter collisions. Deexcitation proceeds through many Auger and radiative transitions [1,2]. Since fluorescent yields for M-shell vacancies in gold are small (<0.1) [17], Auger transitions dominate the deexcitation of hollow atoms inside the solid.

UV photons and the few x rays that are emitted per SHCI [10] pass through the contact layer with little interaction and are absorbed in the depletion region where they produce energetic electrons which then form electron-hole pairs. Assuming isotropic angular distributions, photon emission into about half of the full solid angle contributes to electronic excitations in the sensitive detector volume.

The transport of energy from Auger electrons is more complicated, because it involves multiple scattering processes. Inelastic mean free paths of, for example, 500 eV electrons in silicon are only a few nm [18]. Distances traveled between elastic collisions are even shorter and result in significant path length increases [18]. Consequently, Auger electrons undergo many collisions, resulting in energy loss and production of higher generations of secondary electrons with a gradual decrease of mean

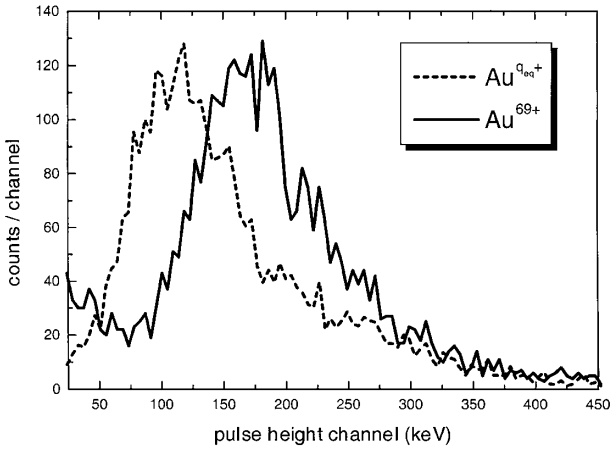

FIG. 1. Pulse height distributions from an ion implanted silicon detector for gold ions in charge state equilibrium ($q_{eq} \approx 1.6+$) and Au^{69+} ions with kinetic energies of 447 keV.

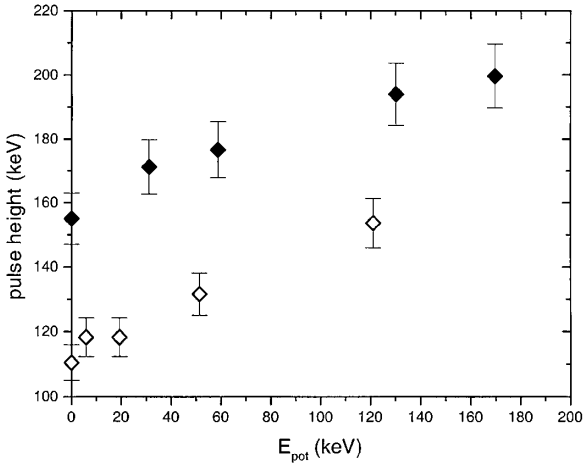

FIG. 2. Mean pulse heights as a function of potential energy for xenon (open) and gold ions (solid) with kinetic energies of 308 keV (xenon) and 447 keV (gold).

energies [19]. This cascade multiplication process comes to a halt when the mean energy of electrons drops below about 3.67 eV, the average energy for the creation of an electron-hole pair in silicon at room temperature. Because the mean free paths are so much smaller than the thickness of the contact layer, most of the energy from Auger electrons is deposited in the contact layer. In the absence of an external electric field, low energy electrons diffuse through the contact layer [14]. Along their path, they can recombine with impurity ions or holes in the valence band [20]. Finally, electrons reach the depletion region were they create electron-hole pairs if their energy is still high enough (i.e., larger than about 3.67 eV). Supported also by the results from studies of secondary electron mission discussed below, we conclude that the majority of electrons that reach the depletion region has lower energies than the minimum energy required for electron-hole pair formation. These low energy electrons are rapidly swept to the collection electrode in the applied electric field. In a conventional solid target, rather than a detector, electrons thermalize along their diffusion paths and dissipate their energy to the lattice [21].

The contribution to the pulse of collected charge from transfer of kinetic energy is given by $E_1(q) = E_{\mathrm{kin}} - E_c(q) - E_n$. Where $E_c(q)$ is the energy lost in the contact layer through—charge dependent—inelastic and elastic energy loss processes, and E_n is the nonelectronic loss to crystal damage and lattice vibrations in the sensitive device layer. We determine $E_1(q)$ by measuring pulse heights for projectiles in charge-state equilibrium and include a small correction for preequilibrium energy loss enhancements in the contact layer [3].

Au^{69+} ions deposit a potential energy of 169.6 keV into the target. The mean pulse height for Au^{69+} ions with a kinetic energy of 447 keV corresponds to an energy of 200 ± 10 keV. For gold ions in charge-state equilibrium and at the same kinetic energy, the value is 155 ± 8 keV. When subtracting this baseline value, we correct for preequilibrium energy loss enhancement in the first few nanometers of the contact layer [3,16]. Because of this, Au^{69+} ions reach the sensitive device volume with a slightly lower kinetic energy than initially low charge-state gold ions. We estimate this effect using data from carbon foils [3] and find a pulse height increase of 59 keV due to deposition of potential energy by Au^{69+}. For Xe^{52+} the value is 49 keV. This fraction of 35% (40% for Xe^{52+}) is by far the largest part of the initially available potential energy that has been traced.

From x-ray emission studies [10], we estimate that about one M-shell x ray with an energy of $\sim$4 keV is detected per Au^{69+}, and subtract this value from the 59 keV. Emission of UV photons has not yet been quantified for SHCI-solid interactions, and we suppose that their contribution is small compared to the contribution from x rays. This assumption is founded in the observation or small fluorescent yields for transitions in outer shells [17]. In consequence of this estimate, we find that the pulse of collected charge from deposition of potential energy is dominated by low energy electrons that have diffused into the depletion region with a small contribution from electron-hole pairs that were formed in the depletion region by UV photons, x rays, and energetic electrons.

The number of electrons collected in the detector following the impact of individual projectiles, i.e., the detector pulse heights, were converted to an energy scale using the fact that the average energy for creation of an electron-hole pair in silicon at room temperature is about 3.67 eV [13]. Reversing this conversion, we can estimate that some 15 000 low energy electrons diffuse into the depletion region following deexcitation of Au^{69+}. In contrast, only a few hundred electrons are emitted into the vacuum [6–8]. This finding is surprising because SHCI equilibrate and deposit their potential energy very close to the surface, i.e., within a depth of about 5 nm [3]. Most of the emitted secondary electrons have energies below 20 eV and only very few Auger electrons were observed for SHCI with impact velocities of 4×10^5 m/s [6]. Our results indicate that the majority of Auger electrons lose most of their energy in many elastic and inelastic collisions before reaching the surface [9,19]. Higher generations of secondary electrons arrive at the surface with energies too low to overcome the surface barrier [19,22]. Instead, they recombine at the surface or they are reflected back into the solid [22]. The minimum energy required for an electron to escape from the SiO_2 conduction band into the vacuum, i.e., the electron affinity, is only 0.9 eV. However, emission of a few hundred electrons from an area of about 1 nm^2 increases the effective barrier height locally in this insulator with relatively low hole mobility [7,23,24]. The extent of this increase is currently not well known. The energy needed for transmission of the Si-SiO_2 barrier is 3.1 eV [22].

Several recombination processes can attenuate the number of electrons along their path through the contact layer. Recombination with impurity ions does not contribute strongly, because electrons in p-type silicon and at an acceptor concentration of $\sim 4 \times 10^{19}$ cm^{-3} have carrier lifetimes and attenuation lengths of about 8 ns and 2 μm, respectively [20]. A more important attenuation channel could stem from the high ionization density of target atoms surrounding the deexciting projectile. A "plasma effect"—well known for fast heavy ions [25]—could increase electron-hole recombination in the vicinity of deexciting projectiles significantly. In fact, this effect was the subject of speculation in an early review of interactions of multiply charged ions with solids [26]. Other than for fast, heavy ions, which deposit most of their kinetic energy in the depletion region, no external electric field is active in the contact layer to aid plasma dispersion. Plasma enhanced recombination can produce again secondary electrons and photons, and energy is lost to lattice vibrations [27]. Data in Fig. 2 indicate that the

traced fraction of potential energy does not change significantly with increasing potential energy. In contrast, plasma enhanced recombination should increase with increasing excitation density and manifest itself in a decrease of the number of low energy electrons that can diffuse to the depletion region. On the other hand, x-ray emission also increases when more inner shell vacancies are present in SHCI [17] and x rays are not effected by a plasma surrounding the deexciting SHCI. Consequently, increased x-ray emission can partially compensate losses from plasma enhanced recombination. Higher fluorescent yields could also account for the higher fractions of E_{pot} detected for Xe^{52+} than for Au^{69+}. More precise measurements of absolute x-ray yields are needed to address this question. Given the large number ($\gg q$) of electrons involved in the deexcitation of SHCI, an effect of plasma enhanced recombination is a likely mechanism for energy deposition and loss of secondary electrons in the contact layer. The magnitude of this attenuation effect cannot be quantified from our results.

Two other major channels for deposition of potential energy that await quantification are permanent lattice damage and phonons. Their importance is already indicated by large ablation yields [11,28].

In summary, we have probed the deposition of potential energy of slow, highly charged ions inside of solids with an ion implanted silicon detector. Mean pulse heights increase strongly as a function of potential energy of projectiles. A fraction of 35% to 40% of the potential energies of Au^{69+} and Xe^{52+} ions is traced in electronic excitations more than 50 nm deep inside the target. This amount of energy corresponds to diffusion of about 15 000 low energy electrons into the depletion region of the detector. In contrast, just a few hundred electrons are emitted into the vacuum and only about 10% of the potential energy has been traced in emitted secondaries.

The authors gratefully acknowledge the excellent technical support at the LLNL EBIT facility provided by D. Nelson and E. Magee. This work was performed under the auspices of the U.S. Department of Energy by Lawrence Livermore National Laboratory under Contract No. W-7405-ENG-48.

*Email address: Schenkel2@LLNL.GOV

[1] D. H. Schneider and M. A. Briere, Phys. Scr. **53**, 228 (1996), and references therein.
[2] A. Arnau *et al.*, Surf. Sci. Rep. **27**, 113 (1997), and references therein.
[3] T. Schenkel *et al.*, Phys. Rev. Lett. **79**, 2030 (1997); **78**, 2481 (1997).
[4] T. Schenkel *et al.*, J. Vac. Sci. Technol. A **16**, 1384 (1998); A. V. Hamza *et al.*, *ibid.* **17**, 303 (1999).
[5] T. Schenkel *et al.*, J. Vac. Sci. Technol. B **16**, 3298 (1998); J. D. Gillaspy *et al.*, *ibid.* **16**, 3294 (1998).
[6] J. W. McDonald *et al.*, Phys. Rev. Lett. **68**, 2297 (1992).
[7] T. Schenkel *et al.*, Nucl. Instrum. Methods Phys. Res., Sect. B **125**, 153 (1997).
[8] F. Aumayr *et al.*, Phys. Rev. Lett. **71**, 1943 (1993).
[9] D. Niemann *et al.*, Phys. Rev. Lett. **80**, 3328 (1998).
[10] R. Schuch *et al.*, Phys. Rev. Lett. **70**, 1073 (1993); M. W. Clark *et al.*, Phys. Rev. A **47**, 3983 (1993).
[11] T. Schenkel *et al.*, Phys. Rev. Lett. **80**, 4325 (1998); **81**, 2590 (1998); G. Schiwietz *et al.*, Radiat. Eff. Defects Solids **127**, 11 (1993); T. Sekioka *et al.*, Nucl. Instrum. Methods Phys. Res., Sect. B **146**, 172 (1998).
[12] Detector from the EG&G Ortec ULTRA™ series. Particle implanted and passivated silicon detectors are silicon based diode structures developed from the well-know surface barrier detectors by substitution of the front metal contact layer (a few hundred nm thick) with a much thinner (50 nm) layer of boron implanted silicon.
[13] E. Steinbauer *et al.*, Nucl. Instrum. Methods Phys. Res., Sect. B **85**, 642 (1994).
[14] T. Cho *et al.*, J. Appl. Phys. **72**, 3363 (1992); H. O. Funsten *et al.*, IEEE Trans. Nucl. Sci. **44**, 2561 (1997).
[15] J. F. Ziegler, J. P. Biersack, and U. Littmark, *The Stopping and Range of Ions in Solids* (Pergamon Press, New York, 1985); http://www.research.ibm.com/ionbeams/
[16] B. Rosner *et al.*, Nucl. Instrum. Methods Phys. Res., Sect. B **42**, 325 (1989).
[17] W. Bambynek *et al.*, Rev. Mod. Phys. **44**, 716 (1972).
[18] Y. F. Chen *et al.*, J. Phys. D **25**, 262 (1992).
[19] R. A. Baragiola, Nucl. Instrum. Methods Phys. Res., Sect. B **78**, 223 (1993).
[20] I.-Yun Leu and A. Neugroschel, IEEE Trans. Electron Devices **40**, 1872 (1993).
[21] M. Inokuti, Appl. Radiat. Isot. **42**, 979 (1991).
[22] M. V. Fischetti *et al.*, J. Appl. Phys. **78**, 1058 (1995).
[23] T. Schenkel, doctoral thesis, Johann Wolfgang Goethe Universität Frankfurt/M, 1997 (unpublished).
[24] H. Jacobsson and G. Holmen, J. Appl. Phys. **74**, 6397 (1993).
[25] E. C. Finch *et al.*, Nucl. Instrum. Methods **163**, 467 (1979), and references therein.
[26] S. Datz, Phys. Scr. **T3**, 79 (1983).
[27] W. E. Drummond and J. L. Moll, J. Appl. Phys. **42**, 5556 (1971).
[28] M. Sporn *et al.*, Phys. Rev. Lett. **79**, 945 (1997).